Published in final edited form as:
Bioconjug Chem. 2006 ; 17(6): 1551–1560. doi:10.1021/bc060156+.

Influence of the Linker on the Biodistribution and Catabolism of Actinium-225 Self-Immolative Tumor-Targeted Isotope Generators

Christophe Antczak, **Jaspreet S. Jaggi**, **Clare V. LeFave**, **Michael J. Curcio**, **Michael R. McDevitt**, and **David A. Scheinberg***
Department of Molecular Pharmacology and Chemistry, Memorial Sloan Kettering Cancer Center, New York, NY 10021

Abstract

Current limitations to applications of monoclonal antibody (mAb) targeted isotope generators in radioimmunotherapy include the low mAb labeling yields and the non-specific radiation of normal tissues by non-targeted radioimmunoconjugates (RIC). Radiotoxicity occurs in normal organs that metabolize radiolabeled proteins and peptides, primarily liver and kidneys, or in radiosensitive organs with prolonged exposure to the isotope from the blood, such as the bone marrow. Actinium-225 nanogenerators also have the problem of released alpha emitting daughters. We developed two new bifunctional chelating agents (BCA) in order to address these issues. Thiol-maleimide conjugation chemistry was employed to increase the efficiency of the mAb radiolabelings by up to 8 fold. In addition, one bifunctional chelating agent incorporated a cleavable linker to alter the catabolism of the alpha particle emitting mAb conjugate. This linker was designed to be sensitive to cathepsins to allow release and clearance of the chelated radiometal after internalization of the radioimmunoconjugate into the cell. We compared the properties of the cleavable conjugate (mAb-DOTA-G3FC) to non-cleavable constructs (mAb-DOTA-NCS and mAb-DOTA-SH). The cleavable RIC was able to release 80% of its radioactive payload when incubated with purified cathepsin B. The catabolism of the constructs mAb-DOTA-G3FC and mAb-DOTA-NCS was investigated *in vitro* and *in vivo*. RIC integrity was retained at 85% over a period of 136 hours in mouse serum *in vivo*. Both conjugates were degraded over time inside HL-60 cells after internalization and in mouse liver *in vivo*. While we found that the rates of degradation of the two RICs in those conditions were similar, the amounts of the radiolabeled product residues were different. The cleavable mAb-DOTA-G3FC conjugate yielded a larger proportion of fragments below 6kDa in size in mouse liver *in vivo* after 12 hours than the DOTA-NCS conjugate. Biodistribution studies in mice showed that the mAb-DOTA-G3FC construct yielded a higher liver dose and prolonged liver retention of radioactivity compared to the mAb-DOTA-NCS conjugate. The accumulation in the liver seemed to be in part caused by the maleimide functionalization of the antibody, since the non-cleavable mAb-DOTA-SH maleimide-functionalized control conjugate displayed the same biodistribution pattern. These results provide an insight into the catabolism of RICs, by demonstrating that the release of the radioisotope from a RIC is not a sufficient condition to allow the radioactive moiety to clear from the body. The excretion mechanisms of radiolabeled fragments seem to constitute a major limiting step in the chain of events leading to their clearance.

*corresponding author: D.A. Scheinberg, 1275 York Avenue, box 531, Tel: 646-888-2190 ; Fax: 646-422-0296, E-mail: d-scheinberg@ski.mskcc.org.

INTRODUCTION

In hematopoietic malignancies, the accessibility of tumor cells in the blood, marrow, spleen and lymph nodes enables rapid targeting of specific antibodies. Several antigens have been identified that allow selective targeting of neoplastic hematopoietic cells while sparing other necessary hematopoietic lineage and progenitor cells. One of the most suitable targets for myeloid leukemias is CD33, an antigen whose expression is restricted to myelogenous leukemias and myeloid progenitor cells. This marker is absent from other normal tissues or ultimate bone marrow stem cells (1–4). The antibody HuM195, humanized version of the antibody M195 directed against CD33, has been developed and characterized by our group (5). M195 showed targeting to leukemia cells in humans (6) with the majority of the bound IgG being internalized into target cells in vivo (7,8). Based on this biology and pharmacokinetics, it has been proposed that mAb tagged with short-lived nuclides emitting short-ranged, high linear energy transfer (LET) alpha particles may be effective in therapy (9). These short ranged particles may be capable of single cell kill while sparing bystanders. High LET alpha emitters used in radioimmunotherapy include Bismuth-212 (10–12) and -213 (13–15), Astatine-211 (16), and Actinium-225. This latter isotope is an *in vivo* isotope generator, in that it has a long (10 day) half-life and decays via alpha emission through 3 short-lived atoms, each of which yields an alpha particle (12,14). Previous work in our laboratory led to the synthesis, purification and analysis of ^{225}Ac stably bound to the IgG via a bifunctional macrocyclic chelator DOTA (1,4,7,10-tetraazacyclododecane-1,4,7,10-tetraacetic acid) (15). These constructs specifically killed leukemia and cancer cells at becquerel (picocurie) levels in vitro. Injection of rodents bearing disseminated human lymphoma or solid carcinoma with single courses of the constructs at kilobecquerel (nanocurie) levels induced tumor regression and prolonged survival in a substantial fraction of animals without toxicity (15,17,18).

A first limitation to the use of targeted ^{225}Ac isotope generators is the poor yield of labeled antibody (19). Chelation of Ac-225 stably under physiological conditions requires the use the macrocyclic chelator DOTA with all four carboxylic groups available (Antczak et al., unpublished data). However, heating to 60°C is necessary for complete and stable ^{225}Ac chelation by DOTA, a condition that is unsuitable for retention of mAb function (19). Therfore, a two-step procedure was developed to label the antibodies (19). The first step consisted of the chelation of ^{225}Ac by the bifunctional chelating agent DOTA-NCS **1** (Scheme 1). A low yield second step of the process was the reaction of the ^{225}Ac-DOTA-NCS **2** with the IgG. HPLC studies showed that the first step largely degrades the isothiocyanate moiety required for the labeling of the antibody in the second step, thus reducing product yields (data not shown). Therefore, we based our new BCAs on novel thiol-based BCAs following the assumption that thiol groups would be more stable than isothiocyanates during the first step of the labeling process.

Another limitation to a more general application of tumor-targeted ^{225}Ac nanogenerators is the excessive radiation of normal tissues by the RIC. With the exception of antibodies targeting leukemias, most (>99%) of the injected antibody dose remains circulating in the blood or is not associated with the target tumor. The prolonged circulation time of untargeted antibodies, typically days to weeks, results in radiation exposure of normal organs that catabolize or retain proteins and peptides, primarily liver and kidneys (20,21). In the case of *in vivo* generators, an additional major potential obstacle to their safe use is the sequential release of 3 unchelated alpha emitting daughter atoms following initial decay of the generator. Uptake into organs such as the kidney or the liver could induce toxicity (22).

One attractive approach to overcome the long circulation time of untargeted radioimmunoconjugates is the development of BCAs that allow conditional release of the chelated radioactive payload. The introduction of a cleavage site in the linkage between the

radiochelate and the mAb is meant to permit the release of a low molecular weight radiochelate from its carrier mAb and its subsequent rapid clearance once the radioconjugate has accumulated in metabolizing organs. The chelated radiometal then rapidly clears the body through the kidneys, thereby reducing toxicity. This strategy has been attempted using disulfide, ester, tartramide, and peptide bonds (23,24). An optimal linker should 1) link the carrier mAb to the radiochelator without impairing the functionality of either; 2) provide a stable linkage in circulation; and 3) degrade under specific conditions. Stability in circulation has proven to constitute a particularly important factor for success using this strategy. Perhaps for this reason, peptide linkers, which are usually more stable than esters and disulfides in serum, have been most successful in RICs and in the design of antibody-drug conjugates (ADC) (25,26). The most extensively studied peptide linkers are sensitive to cathepsins. More precisely, ADCs incorporating the dipeptide valine-citrulline have been shown to enter the target cells and migrate to the lysosomes, where they release their drug specifically under the action of cysteine proteases (27).

The most advanced strategy for the release of a radionuclide from a RIC is the one followed by DeNardo et al., based on cathepsin-sensitive peptide linkers. Based on the hypothesis that intrahepatocyte cathepsins are responsible for most of the protein metabolism in hepatic lysosomes, a BCA was designed to incorporate a specific cathepsin B cleavage site. Even though human tumors express cathepsin B (28), studies from DeNardo et al. have demonstrated that the dose achieved at the xenograft after treatment with four cathepsin B labile radioconjugates was comparable to that achieved with a non-cleavable control. This remained true for two different antibodies and for two human maligancies (an adenocarcinoma and a lymphoma) (29). The cathepsin B-sensitive conjugate glycylglycylglycyl-L-*p*-isothiocyanatophenylalanine-Lym-1 demonstrated great stability in human serum. This cleavable construct was compared to a non-cleavable construct in human breast cancer xenografts, and a 30 to 70% decrease in the liver dose and a slightly increased tumor dose was observed (29,30). In patients with prostate and breast cancer, the pharmacokinetics and tumor dose were similar for both cleavable and non-cleavable RICs, except for about a 30% decrease in the mean dose to the liver with the cleavable linker (31). In another clinical study with patients with breast and prostate cancer, the liver dose was consistantly lower with the cleavable RIC compared to a non-cleavable conjugate, while the tumor dose was not significantly affected by the linker. (32). Therefore, we applied a cathepsin-sensitive linker strategy to the ^{225}Ac nanogenerators.

EXPERIMENTAL PROCEDURES

Radionuclides, reagents, and monoclonal antibodies

The ^{225}Ac was obtained from Oak Ridge National Laboratory (Oak Ridge, TN) as a nitrate salt. The ^{225}Ac salt was dissolved in 0.15M Optima grade HCl (Fisher Scientific, Pittsburgh, PA). Metal-free water (MFW) used for this and all other solutions was obtained from a Purelab Plus system (US Filter Corp., Lowell, MA) and was sterile filtered. The parent ^{225}Ac activity was measured when it was in secular equilibrium with its daughters using a drop well dose calibrator (CRC-17; E.R. Squibb and Sons, Inc., Princeton, NJ) set at 775 and the reading multiplied by 5.

The chelating agent DOTA-NCS **1**, 2-(*p*-isothiocyanatobenzyl)-1,4,7,10-tetraazacyclododecane-1,4,7,10-tetracetic acid, was obtained from Macrocyclics (Dallas, TX). The heterobifunctional linker LC-SMCC and 2-mercaptoethylamine (2-MEA) were provided by Pierce (Rockford, IL). Chemicals used in the radiolabeling and purification steps were ACS reagent grade or better. Dithiothreitol (DTT), Tetramethylammonium acetate (TMAA), L-ascorbic acid (AA), sodium carbonate (Na_2CO_3), dimethylformamide (DMF), triethylamine (Et_3N), trishydroxymethylaminomethane hydrochloride (Tris-HCl), Triton X-100,

trifluoroacetic acid (TFA), acetonitrile (CH_3CN) and ethylenediamine tetraacetic acid (EDTA) were obtained from Sigma-Aldrich (Saint Louis, MO). Sulfur-35 radiolabeled cysteine was provided by PerkinElmer (Wellesley, MA). Bovine spleen cathepsin B (E.C. 3.4.22.1), was obtained from Sigma-Aldrich. The protease inhibitor cocktail was provided by Roche Diagnostics Gmbh (Mannheim, Germany). The cation exchange resin Sephadex C-25 was purchased from Amersham Biosciences (Piscataway, NJ). Human serum albumin (HSA) (Swiss Red Cross, Bern, Switzerland) and 0.9% NaCl (Abbott Laboratories, North Chicago, IL) were used as received. A 10DG desalting column (Bio-Rad, Hercules, CA) was used for RIC purification.

The cell line HL-60 was obtained from the ATCC (catalog# CCL-240) and was cultured following the ATCC recommendations. The humanized murine monoclonal antibody HuM195 directed against the cell surface myelomonocytic differentiation antigen CD33 was generously provided by Protein Design Laboratories (Sunny View, CA). The mouse monoclonal antibody SJ25C1 directed against the CD19 antigen present on human B lymphocytes was provided by the monoclonal antibody core facility of the Sloan-Kettering Institute.

HPLC

Reversed phase HPLC was performed using a Beckman Coulter System Gold Bioessential HPLC, equipped for analytical studies with a Varian C18 Inertsil ODS-3 5μ 250×4.6mm column, and with a Varian C18 Inertsil ODS-3 5μ 250×10mm column for semi-preparative runs. Detection of the peaks was performed using a Beckman Coulter 168 diode array detector at 220 nm. Data was analyzed using the system's 32 Karat software.

Synthesis of 3-Mercapto-2-(3-phenyl-2-{2-[2-(2-{3-[2-*p*-(1,4,7,10-tetraazacyclododecane-1,4,7,10-tetraacetic acid)benzyl]-thioureido}-acetylamino)-acetylamino]-acetylamino}-propionylamino)-propionic acid (3)

To a solution of peptide GGGFC (16.5 mg, 37.6 μmol) and Et_3N (22 μL, 219.1 μmol) in dry DMF, a solution of DOTA-NCS **1** (17.2 mg, 31.3 μmol) in dry DMF was slowly added. After one hour reaction at room temperature the product DOTA-G3FC **3** was purified by semi-preparative reversed phase HPLC. The mobile phases consisted of A, 0.1% (v/v) trifluoroacetic acid (TFA) in water, and B, 0.1% TFA in acetonitrile (CH_3CN). The reaction mixture was solubilized in mobile phase A and injected for a 30 min run at 5.0 mL/min at room temperature. The column was previously equilibrated in eluent A with 5% eluent B. The gradient was 5–20% B in 20 min, 20–90% B in 10 min. After lyophilization, the desired product **3** was isolated as a white powder (26.5 mg, 26.8 μmol, 86% yield) and stored under vacuum. Analytical HPLC using the same gradient gave a single peak. HRMS (ESI): *m/z* 496.1860 $[M+2H]^{++}$; calcd for $C_{42}H_{58}N_{10}O_{14}S_2$ 990.3575; found 990.3563.

Synthesis of 2-*p*-(2-mercaptoethylthioureido)benzyl-(1,4,7,10-tetraazacyclododecane-1,4,7,10-tetraacetic acid) (4)

To a solution of 2-mercaptoethylamine (2-MEA) (1.3 mg, 11.5 μmol) and Et_3N (1.8 μL, 17.9 μmol) in dry DMF was slowly added a solution of DOTA-NCS **1** (4 mg, 7.3 μmol) in dry dimethylformamide (DMF). After one hour reaction at room temperature the product **4** was purified by semi-preparative reversed phase HPLC as previously described for compound **3**. After lyophilization, the desired compound **4** was isolated as a white powder (3.9 mg, 6.19 μmol, 85% yield) and stored under vacuum. Analytical HPLC using the same gradient gave a single peak. HRMS (ESI): *m/z* 629.2434 $[M+H]^+$; calcd for $C_{26}H_{40}N_6O_8S_2$ 628.2349; found 628.2356.

Functionalization and Characterization of Maleimide-Antibodies

The heterobifunctional linker LC-SMCC (0.375 mg, 833 nmol) was solubilized just prior use in DMSO, and added to 1 mL of the antibody solution in PBS (5 mg, 33.3 nmol). The pH was adjusted to 7.0 by adding a few microliters of a 200 mM Na_2CO_3 solution to the reaction mixture, and the reaction was carried out over 2 hours at 24°C. The modified antibody was purified by size-exlusion chromatogaphy (10DG desalting column, Bio-Rad) in degassed PBS EDTA 5mM, pH 6.4. Protein concentration was performed using Microcon YM-50 centrifugal filter devices (Millipore) in order to reach 3 to 5 mg/mL. The protein concentration was determined using the Bradford assay (Bio-Rad) before storage at −80°C. The extent of maleimide functionalization was determined by trace-labeling with ^{35}S-labeled cysteine. The antibody solution in PBS EDTA 5 mM, pH 6.4 (100 μL, 0.3 mg, 2 nmol) was mixed with cysteine (0.07 mg, 400 nmol) containing trace amounts of ^{35}S-cysteine. The pH was adjusted to 7.0 by adding a few microliters of a 200 mM Na_2CO_3 solution, and after 30 minutes at room temperature, the protein was purified from the low molecular weight content by size-exclusion chromatography. After determination of the protein concentration, an aliquot was counted in a β scintillation counter (Beckman LS6000 IC), and by comparison with an aliquot of the ^{35}S-cysteine/cold cysteine solution, the total amount of cysteine bound to the protein was calculated. Using the protein concentration, the amount of maleimide residues per antibody was determined.

Preparation of Radioimmunoconjugates

The chelation of the radiometal during the first step to yield the chelates **2, 7**, and **8** was performed as follows. All the reagent solutions were degassed by sonication under vacuum just prior use. Depending on the scale of the subsequent conjugation reaction, a few microliters of $^{225}Ac(NO_3)_3$ dissolved in 0.15M HCl or $^{111}InCl_3$ at 0.1 mCi/mL were added to 50 μL of 2M tetramethylammonium acetate (TMAA). To this solution was added 20 μL of 150 g/L ascorbic acid (AA) as a radioprotectant and 50 to 500 μL of the BCA solubilized at 1 to 10 mg/mL in freshly degassed metal-free water (MFW). If necessary, another 50 μL of the TMAA solution was added in order to reach pH 5.5. The pH was checked by testing an aliquot of the reaction mixture using pH test papers in the appropriate range (Micro Essential Laboratory, Inc., NY).The reaction mixture was incubated under argon at 60°C over 30 minutes. The percentage of incorporation of the radiometal by the chelate was determined by loading 1–2 μL of the reaction mixture onto a 1 mL cation exchange resin (Sephadex C-25) equilibrated with 0.9% saline and eluting the column two times with 3 mL of saline. The eluate was collected, and the activity of the eluate and the column measured immediately for ^{111}In and when in equilibrium with its decay products in the case of ^{225}Ac. Chelated radiometals elute, whereas the free radiometals are retained on the column.

The second step of the labeling was achieved by adding 100 μL to 1 mL of the unmodified or maleimide-functionalized antibody in solution with 5mM EDTA (3 to 5 mg/mL) to the reaction mixture. The pH was brought to 8.5 by adding a few microliters of a 200 mM Na_2CO_3 solution. The conjugation was allowed to proceed for 150 min at 37°C. Purification of the conjugate was performed using a 10-DG desalting column using saline with 1% HSA as the mobile phase.

Characterization of the Radioimmunoconjugates

The radiochemical purity of the RICs was determined by instant TLC in triplicate (SG TLC plates; Gelman Sciences Inc., Ann Arbor, MI) using 10 mM EDTA as the mobile phase. The strips were analyzed immediately for detecting ^{111}In or allowed to sit overnight before measuring ^{225}Ac. Analysis was performed using a gas ionization detector (Ambis 4000; Ambis, San Diego, CA). The *Rf* of the radiolabeled antibody was 0 and both the free metal species and metal chelates were characterized by a *Rf* of 1.

The immunoreactivity of the purified RICs was determined by incubating the radiolabeled antibodies with AL67 (CD33-positive) or Daudi (CD33-negative) cells. First, cells were washed twice with ice-cold PBS and then blocked by incubation on ice with 2% rabbit serum. Then 8 ng of the RICs of 1% HSA in PBS was added to 2.5E7 AL67 cells or 5E6 Daudi cells and incubated on ice for 30 min in a final volume of 20 μL. The cells were washed twice with ice-cold-PBS, and the washes were saved and counted along with the cells after 20h.

Radiometal Release by Cathepsin B and in vitro Serum Stability

The cleavable RIC SJ25C1-DOTAG3FC **11** was used for these studies. Assay conditions were chosen to approximate the lysosomal medium. A stock solution of bovine spleen cathepsin B was prepared by dissolving the lyophilized solid at 15 U/mL in the cathepsin buffer, which consisted of 50 mM sodium acetate,1 mM EDTA, pH 4.5. The enzyme was activated just prior use by incubation at 37°C with 50 mM DTT for 30 minutes. The assay was performed at 37° C using 25 μg conjugate, and the final enzyme concentration was 1.5 U/mL in a total volume of 150 μL. The control cathepsin buffer experiment was run in the exact same conditions except no enzyme was added. The serum stability experiment was conducted at 37°C with fresh human or mouse (BALBC/c) serum prepared in the laboratory.. The final serum concentration was 64% in saline, pH 7.6. The radiometal release was assessed by TLC. Preliminary studies using sodium hydroxide as the mobile phase allowed us to determine that the radiometal was released in a chelated form (Rf = 1). Kinetic studies were later performed by TLC using 10 mM EDTA as the mobile phase. The protein bound ^{225}Ac was measured at $Rf = 0$, and expressed as a percentage of the total activity of the strip at equilibrium. Mean values and standard deviations were calculated from triplicate TLC experiments.

Animal Studies

Female BALB/c mice 10 weeks of age were obtained from Taconic (Germantown, NY). The studies were conducted according to the NIH Guide for the Care and Use of Laboratory Animals and were approved by the Institutional Animal Care and Use Committee at Memorial Sloan Kettering Cancer Center.

The mice were anesthetized and then injected i.v. (via the retroorbital venous plexus) with 0.5 μCi labeled antibody. The injected volume was 100 μL. Animals were sacrificed at different time points after injection by carbon dioxide asphyxiation, and the liver was removed. In addition, for the biodistribution studies, samples of blood (by cardiac puncture) and kidneys were removed. The organs were washed in distilled water, dried on gauze, weighed, and the activities of ^{221}Fr (185–250 keV window) and ^{213}Bi (360–480 keV window) were measured using a gamma counter (COBRA II, Packard Instrument Company, Meriden, CT). Samples of the injectate were used as decay correction standards. Percentage injected dose of ^{225}Ac per gram of tissue weight (%ID/g) was calculated for each animal at the time of sacrifice, using the equation described previously (33). The mean %ID/g was determined for each experimental group.

Radiometal Release in Cultured Cells and in vivo

Assessment of RIC integrity was performed by Protein A assay. The Protein A resin (Protein A sepharose CL-4B resin Amersham Biosciences, Piscataway, NJ) was used according to the directions provided by the supplier. The beads were washed 3 times in PBS before use. For each experiment a 100 fold excess beads was used compared to the calculated amount of Protein A necessary to bind the the estimated amount of antibody.

For the cell internalization experiment, 2E6 HL-60 cells per mL were incubated for 30 minutes in RPMI 1640 with 10% fetal bovine serum with 30 ng of conjugate **9** or **11** labeled with ^{225}Ac in a total of 6 mL on ice. Each experiment was conducted in duplicate and data

values were averaged. After 2 washes with cold media, the cells were resuspended at 1E6 cells per mL in fresh media and incubated at 37°C. At different time points, the cells were washed 2 times with cold media and the pellet was lysed for 30 minutes at 4°C in 100 mM NaCl 10 mM Tris-HCl buffer pH 8.0 containing 1% Triton and supplemented with the Roche protease inhibitor cocktail. The Protein A resin in suspension in PBS was then added to the cell lysate and the suspension was agitated for 30 minutes at 4°C. The resin was then separated from the supernatant by quick centrifugation and washed 2 times. The radioactivity was measured in scintillation liquid using a beta counter. The activity in the washes was negligible, and the activity associated to the beads was at least 25-fold superior to background. The antibody-bound activity was expressed as the percentage of the activity bound to the beads compared to the total activity found in the supernatant and associated with the resin.

For the *in vivo* radiometal release experiments, the constructs **9** or **11** labeled with ^{225}Ac (0.1 mCi in saline 1%HSA) were injected IP to 2 groups of 3 Balb/c female mice. At different time points the isolated livers were homogenized on ice in 10 mL of 10mM Tris-HCL buffer at pH 8.0 containing 0.25M sucrose and 1% Triton X100, supplemented with the Roche protease inhibitor cocktail. After pelleting at 12,000 g at 4°C for 10 minutes, the supernatant was submitted to the Protein A beads assay as described above. In order to estimate the size of the antibody fragments carrying the radiolabel, the liver extracts were submitted to size-exclusion chromatography using 10DG columns (Bio-Rad), which have a 6 kDA molecular weight cut-off. This type of column was previously calibrated in the laboratory using the following method. Fractions collected after the purification of the RIC HuM195-DOTA-NCS labeled with ^{225}Ac were analyzed by size exclusion HPLC to determine the volume corresponding to the elution of high molecular weight molecules. The same protocol was later used to analyze the radiolabeled components of the liver homogenates, allowing to seperate the high (>6kDa) and low (<6kDa) molecular weight content.

RESULTS

Design and Synthesis of the Bifunctional Chelating Agents

In order to achieve high labeling yields, we based our conjugation strategy on thiol/maleimide chemistry because thiols would be resistant to the conditions used during the ^{225}Ac chelation step. Since all four carboxylic groups of DOTA need to be available for stable ^{225}Ac chelation, we decided to use the bifunctional DOTA-NCS **1** macrocyclic chelator as the starting material for the synthesis of the new linkers, because its *p*-benzylisothiocyanate moiety is directly linked to the macrocycle backbone rather than to one of the carboxylic groups.

We used a cathepsin B-sensitive linker in the design of our self-immolative nanogenerators on the basis that cathepsin B is a prominent enzyme implicated in the catabolism of proteins in the liver (29–31,34). The cleavable BCA DOTA-glycylglycylglycyl-L-*p*-isothiocyanatophenylalanine used by DeNardo et al. was shown to be cleaved by cathepsin B before the phenylalanine residue (35). This residue was bound to the antibody through a thiourea moiety in the *para* position of the benzyl moiety. We hypothesized that this non-peptidic bond was not required for recognition by the enzyme cathepsin B, and instead we incorporated to our linker a regular phenylalanine residue. A terminal cysteine residue was added in order to provide the reactive thiol for conjugation to the maleimide-functionalized antibody. The synthesis of our cleavable BCA required a single step consisting of coupling the pentapeptide GGGFC to DOTA-NCS (Scheme 1). This was achieved in anhydrous DMF in the presence of triethylamine with a 86% yield ; the resulting product DOTA-G3FC **3** was purified by semi-preparative reversed phase HPLC. Similarly, we synthesized the non-cleavable control BCA DOTA-SH **4** by coupling DOTA-NCS with 2-mercaptoethylamine (2-MEA), with a 85% yield.

Preparation of the Radioimmunoconjugates

Our thiol-maleimide conjugation strategy requires the functionalization of the antibody with a maleimide moiety, which was readily achieved through the use of the commercially available bifunctional linker LC-SMCC (Scheme 2). The long chain (LC) version of this reagent was preferred in order to reduce the possible steric hindrance provided by the proximity of the antibody, therefore allowing maximum accessibility of the enzyme cathepsin to the linker. The protocol allowed derivatization of the antibody with a reproducible amount of maleimides. A 25-fold molar excess of LC-SMCC per antibody yielded about 8 moles maleimide per mole of HuM195 antibody (7.7±0.9; n=8). Purification of the functionalized antibody **5** was achieved by size-exclusion chromatography. This functionalization method was successfully applied to two different antibodies: HuM195 and SJ25C1. Using similar conditions as the one optimized for HuM195 led to the functionalization of SJ25C1 with a reproducible amount of about 8 maleimide moieties per antibody. The degree of maleimide functionalization was assessed by ^{35}S-cysteine labeling of an aliquot of the prepared batch of antibody (Scheme 2). Specific activity was determined on the product, allowing determination of the number of of available maleimides per antibody. The storage buffer (freshly degassed PBS with 5 mM EDTA) at pH 6.4 was chosen because the slightly acidic pH is necessary for the stability of the construct. Upon storage at −80°C in PBS/EDTA at pH 6.4, the functionalized mAbs suffered little loss of their maleimide moiety (1 to 9% over a period of 6 months). The presence of EDTA and the degassing are important for the second step, in order to prevent the oxidation of the reactive thiol on the BCAs **7** and **8**.

The chelation efficiencies of ^{225}Ac by the newly synthesized BCAs to yield the chelates **7** and **8** were similar to those obtained with DOTA-NCS **1**. Metal chelation efficiency was typically 95 to >99% when using a ^{225}Ac:DOTA ratio of 1:5,000 or greater.

The non-cleavable, control RIC mAb-DOTA-NCS **9** (15,19), was prepared using the commercially available BCA DOTA-NCS **1**. After completion of the first step, the reaction of **2** with the antibody afforded the RIC **9** with a radiochemical yield of 5 to 10%. Its radiochemical purity was typically 90% or greater. Previous studies have shown that an average of 5.4 DOTA per antibody are attached (19).

The conjugate mAb-DOTA-SH (**10**) (Scheme 2) was prepared using the novel, non-cleavable BCA DOTA-SH (**4**). We optimized the conditions of the maleimide/thiol conjugation during the second step using the ^{225}Ac chelate DOTA-SH **8**. Increasing the pH up to 8.5 increased the radiochemical yields by up to 2-fold compared to pH 6.8. Similarly, incubating the reaction mixture at 37°C instead of the room temperature increased the efficiency by a factor of 1.8. The stoichiometry of the reaction also constituted an important parameter in the reaction, since using 0.5 molar equivalents of BCA **8** per maleimide instead of a 2:1 DOTA-SH:maleimide ratio increased the radiochemical yield by another 2 fold. When combined, these parameters allowed the labeling of antibodies with ^{225}Ac through the non-cleavable BCA **8** with radiochemical yields ranging from 30 to 40%. The purity of those constructs was 93% and greater, as assessed by thin layer chromatography (TLC). When applied to the labeling of antibodies with the cleavable BCA **7** and ^{225}Ac, those conditions afforded the same range of yields and purities.

Characterization of the RICs *in vitro*

The immunoreactivity of the three different constucts HuM195-DOTA-NCS **9**, HuM195-DOTA-SH **10**, and HuM195-DOTAG3FC **11** labeled with ^{225}Ac were tested on the CD33-positive AL67 cells. All conjugates were active with immunoreactivities of 93%, 87% and 82%, respectively. The amount of construct bound to the control CD33-negative Daudi cells ranged between 1 and 2%. Therefore, neither the maleimide functionalization of the mAb

HuM195 or its coupling to the newly synthesized BCAs significantly affected the immunoreactivity or specificity of the antibody *in vitro*.

The next step in the evaluation of the cleavable construct mAb-DOTA-G3FC **11** consisted of verifying the recognition of the inserted linker as a substrate of cathepsin B *in vitro*. As assessed by TLC, the construct released ^{225}Ac in a chelated form over time when incubated with purified cathepsin B at 37°C (Figure 1). The drug cleavage half-life was about 150 minutes, and up to 80% of its radioactive payload was released within 7 hours. As a control, the RIC was incubated in the cathepsin buffer without cathepsin B, in order to test whether the acidic conditions (pH 4.5) were responsible for the degradation of the linker. No significant radioisotope release was observed within 10 hours, indicating that the cleavage of the linker was cathepsin-dependent (Figure 1). We showed that the cathepsin is cleaving the linker, rather than the IgG backbone by conductiong another control, which consisted of analyzing the non-cleavable conjugate SJ25C1-DOTA-NCS **9** in the same conditions. Only about 10% of the conjugated radiometal was released within 10 hours, demonstrating that the degradation observed with the construct SJ25C1-DOTAG3FC 11 was linker-dependent, and did not result of antibody metabolism by cathepsin B during that timeframe (data not shown).

The observed degradation of the RIC in mouse and human serum was lower than 20% over 20 hours at 37°C, indicating that it was stable in these conditions. When the *in vitro* cleavage of the cathepsin-sensitive RIC mAb-DOTA-G3FC (made with either the HuM195 antibody (data not shown) or the mouse SJ25C1 antibody) was tested, no difference in the degradation rate between the two constructs was observed. This indicated that the source of the antibody seemed not to interfere with the enzymatic cleavage of the DOTA-G3FC BCA.

We wanted to investigate whether the self-immolative RIC mAb-DOTA-G3FC was susceptible to degradation after cell internalization *in vitro.* For this purpose we compared the fate of the cleavable HuM195-DOTA-G3FC **11** and of the non-cleavable HuM195-DOTA-NCS **9**, each labeled with ^{225}Ac, in target HL-60 cells. After specific binding at 4°C and internalization at 37°C, both RICs were degraded inside the cells over time, as demonstrated by the increasing failure of the labeled construct to bind Protein A beads (Figure 2A). The rate of degradation of both RICs was similar. This result suggested that both the non-cleavable RIC HuM195-DOTA-NCS **9** and the cathepsin-sensitive RIC HuM195-DOTA-G3FC **11** are susceptible to protein catabolism after cell internalization, presumably inside the lysosomes. As the kinetics of loss of binding to Protein A were similar, it appeared that both constructs were submitted to a protease activity that separated the radiolabel from the Fc portion of the IgG.

Characterization of the RICs *in vivo*

A Protein A bead assay was run on the serum of mice injected with the same constructs labeled with ^{111}In. The experiment showed that all 3 conjugates were stable in mouse serum *in vivo*, since between 80 and 85% of the serum activity was antibody-bound after 136 hours.

The catabolism of the three RICs labeled with ^{225}Ac was investigated *in vivo* after IV injection in mice. Mouse livers from untreated animals were homogenized at different time points, and the integrity of the RICs was assessed using the Protein A bead assay (Figure 2B). As a control, the intact RICs were mixed with a liver homogenate suplemented with a cocktail of protease inhibitors. In these control conditions, 80% of both RICs were able to bind the Protein A beads. In contrast, at 12 and 88 hours after injection, both RICs were significantly degraded since their ability to recognize the beads was reduced to about 10%. Similar to the *in vitro* observation with HL-60 cells, both constructs had their radiolabel separated from a functional Fc at the same rate ..

In order to estimate the size of the fragments carrying the radiolabel, at 12 hours after injection, we passed the liver extracts through a size-exclusion column (10DG). This analysis revealed that 84% (±3%) of the radioactivity was bound to fragments smaller than 6 kDa for the cleavable RIC, whereas those fragments represented only 62% (±3%) for the non-cleavable RIC HuM195-DOTA-NCS.

We then compared the biodistribution in mice of ^{225}Ac after injection of the cleavable RIC HuM195-DOTA-G3FC **11** or of the non-cleavable RIC HuM195-DOTA-NCS **9** (Figure 3). For this study, we included another non-cleavable control construct: HuM195-DOTA-SH **10**. The antibody in the latter conjugate was functionalized with maleimides the same way the degradable RIC **11** was, but the BCA DOTA-SH **4** used for its labeling is not sensitive to cathepsins. The biodistribution study revealed that all 3 constructs cleared from the blood in a similar way, approaching 10 to 14% of the injected dose at 168h. A striking difference, however, was seen in the accumulation into the liver. Both the non-cleavable HuM195-DOTA-SH and the cleavable HuM195-DOTA-G3FC constructs yielded a 2 fold higher liver accumulation at 24h compared to the non-cleavable HuM195-DOTA-NCS conjugate. Their slow clearance from the liver eventually yielded a 3 fold higher liver uptake at 168h. The kidney accumulation for the two maleimide-functionalized constructs **10** and **11** was sligthly lower, probably related to the increased liver uptake. Clearance was observed over time for all constructs.

DISCUSSION

This report describes the synthesis of 2 new BCAs that allow markedly improved yields for the labeling of antibodies with ^{225}Ac. Using the newly synthesized BCAs, chelation yields of 95 to >99% and labeling yields of up to 40% were routinely observed. This result constitutes a dramatic improvement compared to the typical yields using the isothiocyanate-functionalized macrochelator DOTA-NCS **2**, which average 5 to 10% (19). This difference is likely to be attributable to the sensitivity to hydrolysis of DOTA-NCS during the chelating step of ^{225}Ac at 60°C. This hypothesis was in part confirmed by a HPLC stability study, which showed a half-life of DOTA-NCS of 30 minutes in those conditions (data not shown). We therefore demonstrate here that thiol/maleimide chemistry constitutes an alternative conjugation method that is preferrable when a high radiochemical yield is needed with ^{225}Ac. The yields might be further improved with additional process development and optimization.

The pharmacology of an *in vivo* isotope generator is complex. The three alpha-emitting daughters of ^{225}Ac pose a potential threat to injected patients if the elements can not be controlled and cleared quickly. Strategies to decrease exposure to RICs of non-target organs include antibody engineering, pretargeting, extracorporeal depletion, and cleavable conjugates (25). In this article, we describe the design of a self-immolative tumor-targeted isotope nanogenerator. Our intent was to develop a RIC capable of generating 4 high LET alpha particles at the tumor site, and whose radioactive payload can be enzymatically disarmed in order to reduce damage to normal tissues should the RIC not target. The DOTA-G3FC BCA **3** incorporates a cleavage site for the enzyme cathepsin B allowing release of the radiometal from the carrier antibody in a chelated, safe form. The specific degradation of the linker by purified cathepsin B was demonstrated. The chemical half-life of the linker in those conditions was 150 minutes, whereas no significant radiometal release was observed during that timeframe with buffer only. Furthermore, this peptide link proved to be stable in circulation *in vivo*, since the cleavable RIC HuM195-DOTA-G3FC **11** labeled with ^{225}Ac was found intact in mouse serum 136h after injection.

When we investigated the fate of the cleavable RIC **11** after internalization in cultured HL-60 cells, we discovered that its rate of degradation (as measured by retention of the isotope on

Protein A-beads, which requires an intact Fc portion for binding) was similar to the non-cleavable control construct **9**. This result was confirmed *in vivo* in the liver homogenate experiment. A rapid degradation of both constructs occurs in mouse liver, leaving less than 20% conjugate intact 12h after injection. The nature of the degradation, however cannot be determined by this assay. Other groups have reported that radiolabled antibodies are processed after cell internalization. Geissler at al. have shown that following cell surface binding, different radiolabeled antibodies are internalized and degraded in the lysosome (36,37). When injected *in vivo*, a large fraction of a radiolabeled murine antibody against a tumor glycoprotein accumulated in the liver. Its liver uptake is mediated by its Fc portion (38). The same authors observed the conversion in the liver of the ^{111}In-DTPA RIC into small radiolabeled fragments, presumably ^{111}In-DTPA bound to one or a few aminoacids. This hypothesis was confirmed by several groups who identified the *in vivo* metabolite of different ^{111}In-DTPA-NCS labeled proteins as indium-DTPA-lysine (39–41). Therefore, it is likely that the non-cleavable control construct HuM195-DOTA-SCN **9** undergoes a similar process, explaining the degradation we observed after cell internalization *in vitro* and in the liver *in vivo*.

Based on the Protein A assay, the kinetics of degradation observed for the cleavable RIC **11** and the non-cleavable construct **9** were similar within the studied timeframe. However, the Protein A assay does not provide information regarding the way the radiolabeled antibody was degraded, other than reporting the separation of the radiolabel from a functional Fc end of the IgG. We could therefore not rule out the possibility that the degradation of both constructs was qualitatively different, and that the cathepsin-sensitive linker was degraded in addition to the catabolism of the antibody. For this reason we investigated the size of the radiolabeled fragments in the liver. At 12h after injection, the proportion of small radiolabeled fragments (<6kDa) was significantly greater for the cleavable construct, suggesting that additional processing of the linker had occured. It is also likely that a more significant difference may be observed at earlier time points. Indeed, a study using comparable cathepsin-sensitive RICs demonstrated processing of the radiolabeled conjugates in mice liver as early as 30 minutes post injection. In particular, a RIC with a linker incorporating the sequence Gly-Phe-Gly showed little radioactivity associated with the intact antibody and most of the activity associated with the low molecular weight fragments in a gel filtration chromatography experiment after hepatic catabolism (42). Similar to our findings, a study was recently published that describes the unexpected activity of a control immunoconjugate not designed to be able to release an active drug (43). Drug release from this conjugate was shown to take place through mAb degradation. Taken together, these results suggest that the G3FC linker in the cathepsin-sensitive RIC **11** was cleaved *in vivo*, and that catabolism of the antibody backbone took place for both the cleavable and non-cleavable constructs at the same time, obscuring the linker degradation.

When we investigated the biodistribution of the cathepsin-sensitive construct HuM195-DOTA-G3FC **11** in mice, we observed its accumulation in the liver, leading to 2 to 3 fold higher liver uptake compared to the non-cleavable construct HuM195-DOTA-NCS **9**. A different non-cleavable control construct HuM195-DOTA-SH **10** induced a similar liver accumulation of ^{225}Ac in the liver. Since the antibody in this conjugate was functionalized by maleimides the same way as the cleavable construct **11**, it is likely that the functionalization of HuM195 with LC-SMCC was responsible for its increased uptake. It was recently demonstrated that drug-load stoichiometry can significantly influence immunoconjugates pharmacokinetics (44). It is also known that the pI of an antibody or antibody fragment affects its biodistribution (45–47). Therefore, a difference in the number of modifed lysines between the constructs could account for different drug loading and a different overall charge of the conjugates, which could explain the difference in behaviors *in vivo*. Presumably about 8 lysines were modified during maleimide functionalization, which is comparable to the number of lysines derivatized with DOTA-NCS (8–10) using our protocols. However, we cannot rule out

the possibility that the resulting amount of maleimides after reaction with LC-SMCC does not reflect the number of modified lysines, because some maleimide hydrolysis may have occured. Another explanation for the different fate *in vivo* of the two non-cleavable constructs could be a different localization of the radiochelate on the antibody due to the different chemistries used. Catabolism of the conjugates could then produce different labeled fragments, with non-similar excretion properties.. The decreased kidney accumulation consistantly observed for the two maleimide-functionalized constructs **10** and **11** probably resulted from to the increased liver uptake.

Although the cleavable construct HuM195-DOTA-G3FC **11** was demonstrated to be extensively catabolized, the organ distribution profile of the cleavable construct and of the non-cleavable control conjugate HuM195-DOTA-SH **10** were similar. Both constructs showed prolonged retention of the radioactivity in the liver. The lack of accelerated liver isotope clearance by the cathepsin-sensitive linker on the cleavable construct raises questions about the fate of the radioconjugate once inside the liver. We speculate that the accumulation of ^{225}Ac in the liver, which was associated with the treatment with conjugate **11** is the result of an absence of secretion of the radiolabeled metabolites, rather than an absence of cleavage. Lysosomes are known to be highly selective with respect to the release of molecules in the cytoplasm, and accumulation of certain compounds like weak bases results (48). Differences in the catabolism of different radiolabels on antibodies have been observed previously (8). Several authors have reported the accumulation of RIC metabolites in the liver (38), or in their lysosomes (39). Furthermore, not all cathepsin-sensitive linkers in RICs resulted in accelerated liver clearance. For example, while the previously described Ala-Leu-Ala-Leu peptide was beneficial in a daunorubicin conjugate (49), the linker did not significantly increase the liver clearance of a ^{111}In-labeled antibody (50). The authors concluded that the chelates were cleaved off in the liver, but were trapped there(50). The difference in biodistribution with the previously reported result (49) was attributed to the different method used to attach the linker to the antibody, the different number of chelates, and possibly different positions of attachment. In another study, Meares et al. have synthesized various peptide-derivatized DOTA compounds, and selected the best substrates for catepsin B and D (51,52). The most efficiently cleaved peptide sequences *in vitro* were not the linkers leading to the best clearance of the liver *in vivo* (29). This result most likely could be explained by the absence of correlation between rate of linker degradation by purified cathepsin and rate of liver clearance, which depends on other catabolic steps.

Together, these results show that cleavage of a linker by cathepsins is not necessarily the limiting step in the clearance of a self-immolative RIC. We postulate that the catabolism and release of the radiolabeled fragments from liver constitutes a major limiting step in the clearance of RIC metabolites. Therefore, similar cathepsin-sensitive linkers, for example, those reported here and those described by DeNardo et al., could display different biodistributions. Additional support for this hypothesis is derived from work with similar BCAs used to label F(ab')2 antibody fragments with copper, in which slight modifications in the linker structure dramatically influenced the biodistribution and clearance of the radiometal (42). A better understanding of those mechanisms is required for the design of successful self-immolative RIC.

ACKNOWLEDGEMENTS

Christophe Antczak is a Lymphoma Research Foundation Fellow. David A. Scheinberg is Doris Duke distinguished scientist.

The authors thank Dr. Darren Veach, Dr. George Sukenick, Ms. Sylvi Rusli and Ms. Anna Dudkina for helpful assistance with compounds characterization.

This work was supported in part by the NIH grants R01-CA 55349 and CA 33049, the Joseph LeRoy and Ann C. Warner fund, the Lymphoma Foundation, the William and Alice Goodwin Commonwealth Foundation for Cancer Research, and the Sloan Kettering Experimental Therapeutics Center. Actinium-225 was purified at Oak Ridge National Laboratory and was provided by Actinium Pharmaceuticals, Inc.

REFERENCES

1. Scheinberg DA, Tanimoto M, McKenzie S, Strife A, Old LJ, Clarkson BD. Monoclonal antibody M195: a diagnostic marker for acute myelogenous leukemia. Leukemia 1989;3:440–445. [PubMed: 2725060]
2. Tanimoto M, Scheinberg DA, Cordon-Cardo C, Huie D, Clarkson BD, Old LJ. Restricted expression of an early myeloid and monocytic cell surface antigen defined by monoclonal antibody M195. Leukemia 1989;3:339–348. [PubMed: 2716349]
3. Bernstein ID, Singer JW, Andrews RG, Keating A, Powell JS, Bjornson BH, Cuttner J, Najfeld V, Reaman G, Raskind W, et al. Treatment of acute myeloid leukemia cells in vitro with a monoclonal antibody recognizing a myeloid differentiation antigen allows normal progenitor cells to be expressed. J Clin Invest 1987;79:1153–1159. [PubMed: 3470307]
4. Griffin JD, Linch D, Sabbath K, Larcom P, Schlossman SF. A monoclonal antibody reactive with normal and leukemic human myeloid progenitor cells. Leuk Res 1984;8:521–534. [PubMed: 6590930]
5. Co MS, Avdalovic NM, Caron PC, Avdalovic MV, Scheinberg DA, Queen C. Chimeric and humanized antibodies with specificity for the CD33 antigen. J Immunol 1992;148:1149–1154. [PubMed: 1737932]
6. Scheinberg DA, Lovett D, Divgi CR, Graham MC, Berman E, Pentlow K, Feirt N, Finn RD, Clarkson BD, Gee TS, et al. A phase I trial of monoclonal antibody M195 in acute myelogenous leukemia: specific bone marrow targeting and internalization of radionuclide. J Clin Oncol 1991;9:478–490. [PubMed: 1999719]
7. Scheinberg DA, Strand M. Leukemic cell targeting and therapy by monoclonal antibody in a mouse model system. Cancer Res 1982;42:44–49. [PubMed: 6947860]
8. Scheinberg DA, Strand M. Kinetic and catabolic considerations of monoclonal antibody targeting in erythroleukemic mice. Cancer Res 1983;43:265–272. [PubMed: 6571707]
9. Scheinberg DA, Strand M, Gansow OA. Tumor imaging with radioactive metal chelates conjugated to monoclonal antibodies. Science 1982;215:1511–1513. [PubMed: 7199757]
10. Geerlings MW, Kaspersen FM, Apostolidis C, van der Hout R. The feasibility of 225Ac as a source of alpha-particles in radioimmunotherapy. Nucl Med Commun 1993;14:121–125. [PubMed: 8429990]
11. Kaspersen FM, Bos E, Doornmalen AV, Geerlings MW, Apostolidis C, Molinet R. Cytotoxicity of 213Bi- and 225Ac-immunoconjugates. Nucl Med Commun 1995;16:468–476. [PubMed: 7675360]
12. Macklis RM, Lin JY, Beresford B, Atcher RW, Hines JJ, Humm JL. Cellular kinetics, dosimetry, and radiobiology of alpha-particle radioimmunotherapy: induction of apoptosis. Radiat Res 1992;130:220–226. [PubMed: 1574578]
13. Vriesendorp HM, Quadri SM, Andersson BS, Dicke KA. Hematologic side effects of radiolabeled immunoglobulin therapy. Exp Hematol 1996;24:1183–1190. [PubMed: 8765492]
14. McDevitt MR, Barendswaard E, Ma D, Lai L, Curcio MJ, Sgouros G, Ballangrud AM, Yang WH, Finn RD, Pellegrini V, Geerlings MW Jr, Lee M, Brechbiel MW, Bander NH, Cordon-Cardo C, Scheinberg DA. An alpha-particle emitting antibody ([213Bi]J591) for radioimmunotherapy of prostate cancer. Cancer Res 2000;60:6095–6100. [PubMed: 11085533]
15. McDevitt MR, Ma D, Lai LT, Simon J, Borchardt P, Frank RK, Wu K, Pellegrini V, Curcio MJ, Miederer M, Bander NH, Scheinberg DA. Tumor therapy with targeted atomic nanogenerators. Science 2001;294:1537–1540. [PubMed: 11711678]
16. Zalutsky MR, Vaidyanathan G. Astatine-211-labeled radiotherapeutics: an emerging approach to targeted alpha-particle radiotherapy. Curr Pharm Des 2000;6:1433–1455. [PubMed: 10903402]
17. Borchardt PE, Yuan RR, Miederer M, McDevitt MR, Scheinberg DA. Targeted actinium-225 in vivo generators for therapy of ovarian cancer. Cancer Res 2003;63:5084–5090. [PubMed: 12941838]
18. Miederer M, McDevitt MR, Borchardt P, Bergman I, Kramer K, Cheung NK, Scheinberg DA. Treatment of neuroblastoma meningeal carcinomatosis with intrathecal application of alpha-emitting

atomic nanogenerators targeting disialo-ganglioside GD2. Clin Cancer Res 2004;10:6985–6992. [PubMed: 15501978]

19. McDevitt MR, Ma D, Simon J, Frank RK, Scheinberg DA. Design and synthesis of 225Ac radioimmunopharmaceuticals. Appl Radiat Isot 2002;57:841–847. [PubMed: 12406626]
20. Andrew SM, Perkins AC, Pimm MV, Baldwin RW. A comparison of iodine and indium labelled anti CEA intact antibody, F(ab)2 and Fab fragments by imaging tumour xenografts. Eur J Nucl Med 1988;13:598–604. [PubMed: 3350036]
21. Pimm MV, Perkins AC, Baldwin RW. Differences in tumour and normal tissue concentrations of iodine- and indium-labelled monoclonal antibody. II. Biodistribution studies in mice with human tumour xenografts. Eur J Nucl Med 1985;11:300–304. [PubMed: 4076238]
22. Jaggi JS, Seshan SV, McDevitt MR, LaPerle K, Sgouros G, Scheinberg DA. Renal tubulointerstitial changes after internal irradiation with alpha-particle-emitting actinium daughters. J Am Soc Nephrol 2005;16:2677–2689. [PubMed: 15987754]
23. Kukis DL, Novak-Hofer I, DeNardo SJ. Cleavable linkers to enhance selectivity of antibody-targeted therapy of cancer. Cancer Biother Radiopharm 2001;16:457–467. [PubMed: 11789023]
24. Quadri SM, Vriesendorp HM. Effects of linker chemistry on the pharmacokinetics of radioimmunoconjugates. Q J Nucl Med 1998;42:250–261. [PubMed: 9973840]
25. Wu AM, Senter PD. Arming antibodies: prospects and challenges for immunoconjugates. Nat Biotechnol 2005;23:1137–1146. [PubMed: 16151407]
26. Sanderson RJ, Hering MA, James SF, Sun MM, Doronina SO, Siadak AW, Senter PD, Wahl AF. In vivo drug-linker stability of an anti-CD30 dipeptide-linked auristatin immunoconjugate. Clin Cancer Res 2005;11:843–852. [PubMed: 15701875]
27. Sutherland MS, Sanderson RJ, Gordon KA, Andreyka J, Cerveny CG, Yu C, Lewis TS, Meyer DL, Zabinski RF, Doronina SO, Senter PD, Law CL, Wahl AF. Lysosomal Trafficking and Cysteine Protease Metabolism Confer Target-specific Cytotoxicity by Peptide-linked Anti-CD30-Auristatin Conjugates. J Biol Chem 2006;281:10540–10547. [PubMed: 16484228]
28. Berquin IM, Sloane BF. Cathepsin B expression in human tumors. Adv Exp Med Biol 1996;389:281–294. [PubMed: 8861022]
29. DeNardo GL, DeNardo SJ, Peterson JJ, Miers LA, Lam KS, Hartmann-Siantar C, Lamborn KR. Preclinical evaluation of cathepsin-degradable peptide linkers for radioimmunoconjugates. Clin Cancer Res 2003;9:3865S–3872S. [PubMed: 14506184]
30. DeNardo GL, Kroger LA, Meares CF, Richman CM, Salako Q, Shen S, Lamborn KR, Peterson JJ, Miers LA, Zhong GR, DeNardo SJ. Comparison of 1,4,7,10-tetraazacyclododecane-N,N',N'',N'''-tetraacetic acid (DOTA)-peptide-ChL6, a novel immunoconjugate with catabolizable linker, to 2-iminothiolane-2-[p-(bromoacetamido)benzyl]-DOTA-ChL6 in breast cancer xenografts. Clin Cancer Res 1998;4:2483–2490. [PubMed: 9796981]
31. DeNardo SJ, DeNardo GL, Yuan A, Richman CM, O'Donnell RT, Lara PN, Kukis DL, Natarajan A, Lamborn KR, Jacobs F, Siantar CL. Enhanced therapeutic index of radioimmunotherapy (RIT) in prostate cancer patients: comparison of radiation dosimetry for 1,4,7,10-tetraazacyclododecane-N,N',N'',N'''-tetraacetic acid (DOTA)-peptide versus 2IT-DOTA monoclonal antibody linkage for RIT. Clin Cancer Res 2003;9:3938S–3944S. [PubMed: 14506192]
32. Richman CM, Denardo SJ, O'Donnell RT, Yuan A, Shen S, Goldstein DS, Tuscano JM, Wun T, Chew HK, Lara PN, Kukis DL, Natarajan A, Meares CF, Lamborn KR, DeNardo GL. High-dose radioimmunotherapy combined with fixed, low-dose paclitaxel in metastatic prostate and breast cancer by using a MUC-1 monoclonal antibody, m170, linked to indium-111/yttrium-90 via a cathepsin cleavable linker with cyclosporine to prevent human anti-mouse antibody. Clin Cancer Res 2005;11:5920–5927. [PubMed: 16115934]
33. Mirzadeh S, K K, O.A G. The chemical fate of ^{213}Bi-DOTA formed by β-decay of ^{212}Pb(DOTA)2-Radiochimica Acta 1993;60:1–10.
34. Barrett AJ, Kirschke H. Cathepsin B, Cathepsin H, and cathepsin L. Methods Enzymol 1981;80 Pt C:535–561. [PubMed: 7043200]
35. Li M, Meares CF. Synthesis, metal chelate stability studies, and enzyme digestion of a peptide-linked DOTA derivative and its corresponding radiolabeled immunoconjugates. Bioconjug Chem 1993;4:275–283. [PubMed: 8218484]

36. Geissler F, Anderson SK, Press O. Intracellular catabolism of radiolabeled anti-CD3 antibodies by leukemic T cells. Cell Immunol 1991;137:96–110. [PubMed: 1832089]
37. Geissler F, Anderson SK, Venkatesan P, Press O. Intracellular catabolism of radiolabeled anti-mu antibodies by malignant B-cells. Cancer Res 1992;52:2907–2915. [PubMed: 1581908]
38. Jones PL, Brown BA, Sands H. Uptake and metabolism of 111In-labeled monoclonal antibody B6.2 by the rat liver. Cancer Res 1990;50:852s–856s. [PubMed: 2297733]
39. Duncan JR, Welch MJ. Intracellular metabolism of indium-111-DTPA-labeled receptor targeted proteins. J Nucl Med 1993;34:1728–1738. [PubMed: 8410290]
40. Franano FN, Edwards WB, Welch MJ, Duncan JR. Metabolism of receptor targeted 111In-DTPA-glycoproteins: identification of 111In-DTPA-epsilon-lysine as the primary metabolic and excretory product. Nucl Med Biol 1994;21:1023–1034. [PubMed: 9234360]
41. Rogers BE, Franano FN, Duncan JR, Edwards WB, Anderson CJ, Connett JM, Welch MJ. Identification of metabolites of 111In-diethylenetriaminepentaacetic acid-monoclonal antibodies and antibody fragments in vivo. Cancer Res 1995;55:5714s–5720s. [PubMed: 7493333]
42. Novak-Hofer I, Zimmermann K, Schubiger PA. Peptide linkers lead to modification of liver metabolism and improved tumor targeting of copper-67-labeled antibody fragments. Cancer Biother Radiopharm 2001;16:469–481. [PubMed: 11789024]
43. Doronina SO, Mendelsohn BA, Bovee TD, Cerveny CG, Alley SC, Meyer DL, Oflazoglu E, Toki BE, Sanderson RJ, Zabinski RF, Wahl AF, Senter PD. Enhanced activity of monomethylauristatin F through monoclonal antibody delivery: effects of linker technology on efficacy and toxicity. Bioconjug Chem 2006;17:114–124. [PubMed: 16417259]
44. Hamblett KJ, Senter PD, Chace DF, Sun MM, Lenox J, Cerveny CG, Kissler KM, Bernhardt SX, Kopcha AK, Zabinski RF, Meyer DL, Francisco JA. Effects of drug loading on the antitumor activity of a monoclonal antibody drug conjugate. Cancer Res 2004;10:7063–7070.
45. Khawli LA, Glasky MS, Alauddin MM, Epstein AL. Improved tumor localization and radioimaging with chemically modified monoclonal antibodies. Cancer Biother Radiopharm 1996;11:203–215. [PubMed: 10851539]
46. Kim I, Kobayashi H, Yoo TM, Kim MK, Le N, Han ES, Wang QC, Pastan I, Carrasquillo JA, Paik CH. Lowering of pI by acylation improves the renal uptake of 99mTc-labeled anti-Tac dsFv: effect of different acylating reagents. Nucl Med Biol 2002;29:795–801. [PubMed: 12453588]
47. Kobayashi H, Le N, Kim IS, Kim MK, Pie JE, Drumm D, Paik DS, Waldmann TA, Paik CH, Carrasquillo JA. The pharmacokinetic characteristics of glycolated humanized anti-Tac Fabs are determined by their isoelectric points. Cancer Res 1999;59:422–430. [PubMed: 9927057]
48. Ohkuma, S. The lysosomal proton pump. In: Glaumann, H.; Ballard, F., editors. Lysosomes: Their Role in Protein Breakdown. Academic Press; 1987.
49. Trouet A, Masquelier M, Baurain R, Deprez-De Campeneere D. A covalent linkage between daunorubicin and proteins that is stable in serum and reversible by lysosomal hydrolases, as required for a lysosomotropic drug-carrier conjugate: in vitro and in vivo studies. Proc Natl Acad Sci U S A 1982;79:626–629. [PubMed: 6952214]
50. Studer M, Kroger LA, DeNardo SJ, Kukis DL, Meares CF. Influence of a peptide linker on biodistribution and metabolism of antibody-conjugated benzyl-EDTA. Comparison of enzymatic digestion in vitro and in vivo. Bioconjug Chem 1992;3:424–429. [PubMed: 1420442]
51. Peterson JJ, Pak RH, Meares CF. Total solid-phase synthesis of 1,4,7,10-tetraazacyclododecane-N,N', N",N"'-tetraacetic acid-functionalized peptides for radioimmunotherapy. Bioconjug Chem 1999;10:316–320. [PubMed: 10077483]
52. Peterson JJ, Meares CF. Enzymatic cleavage of peptide-linked radiolabels from immunoconjugates. Bioconjug Chem 1999;10:553–557. [PubMed: 10411450]

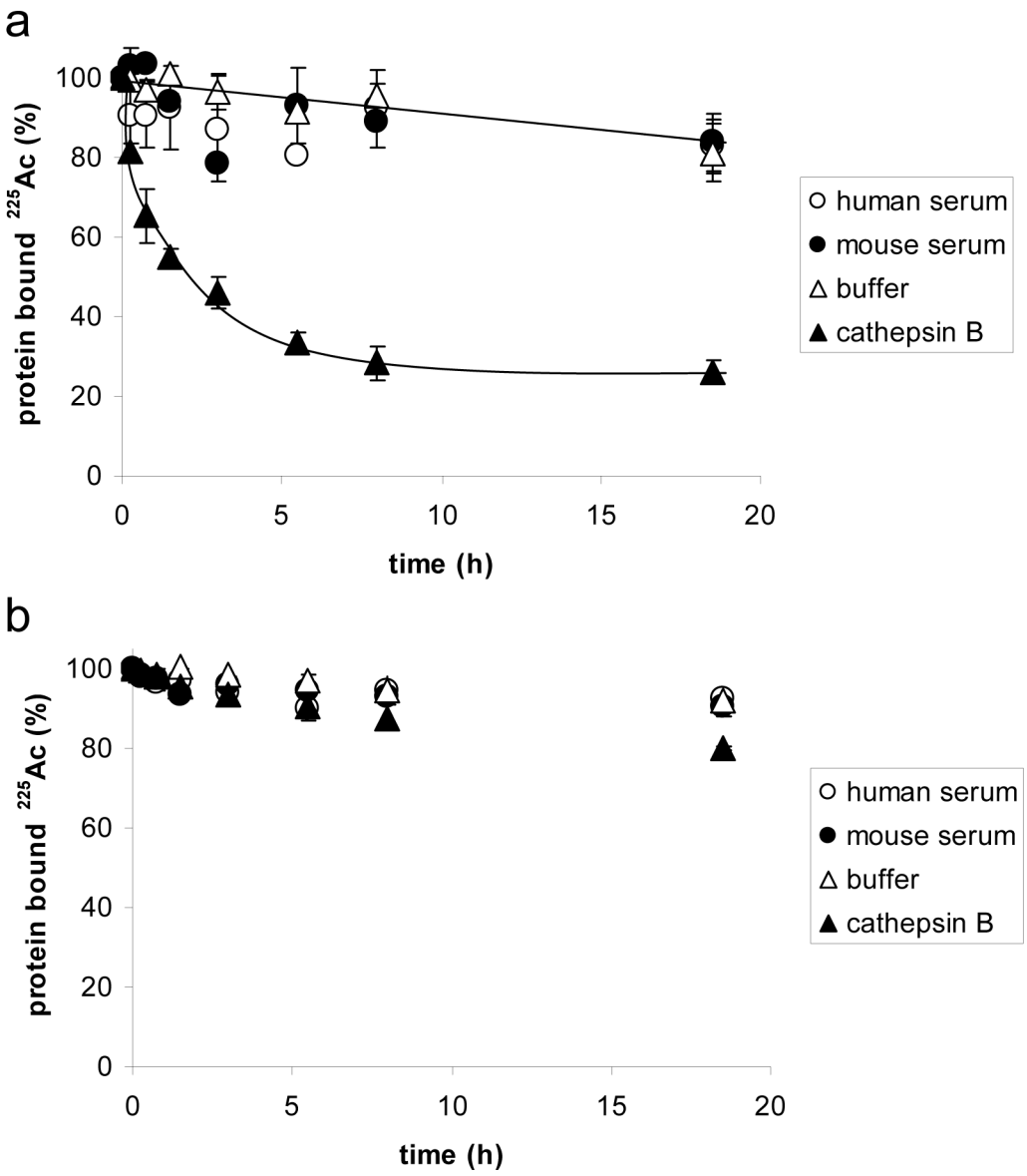

Figure 1.

(a) Cathepsin B-mediated release of chelated ^{225}Ac from the cleavable RIC SJ25C1-DOTA-G3FC **11**. (b) Stability of the non-cleavable RIC SJ25C1-DOTA-NCS **9**. The release of the radiometal from the conjugates was measured at 37°C and assessed by thin layer chromatography.

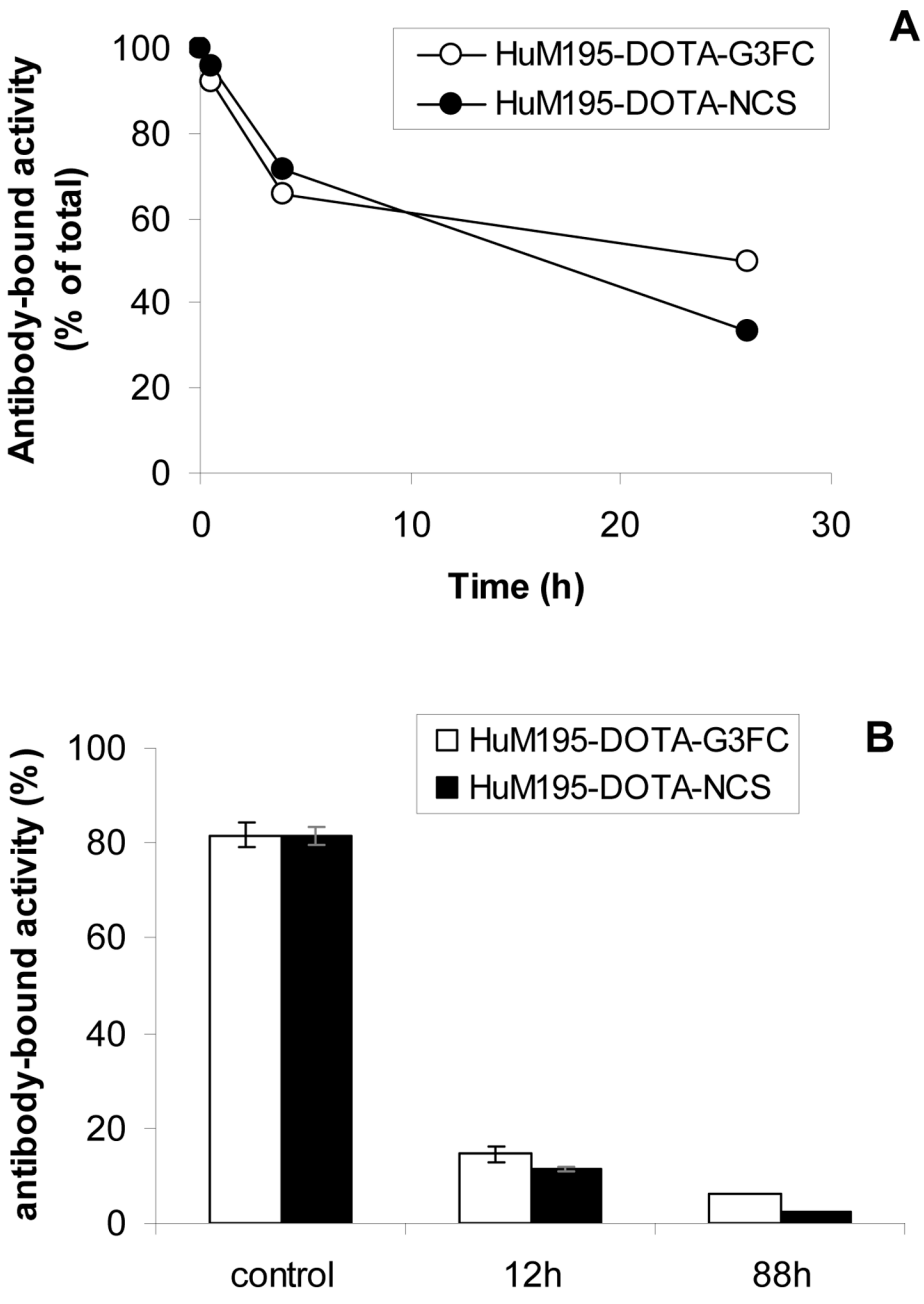

Figure 2.

Comparison of ^{225}Ac release from HuM195-DOTA-G3FC **11** and HuM195-DOTA-NCS **9** after HL-60 cell internalization *in vitro* (A), or in mouse liver *in vivo* (B). The antibody-bound activity was measured after cell homogenization by using Protein A beads.

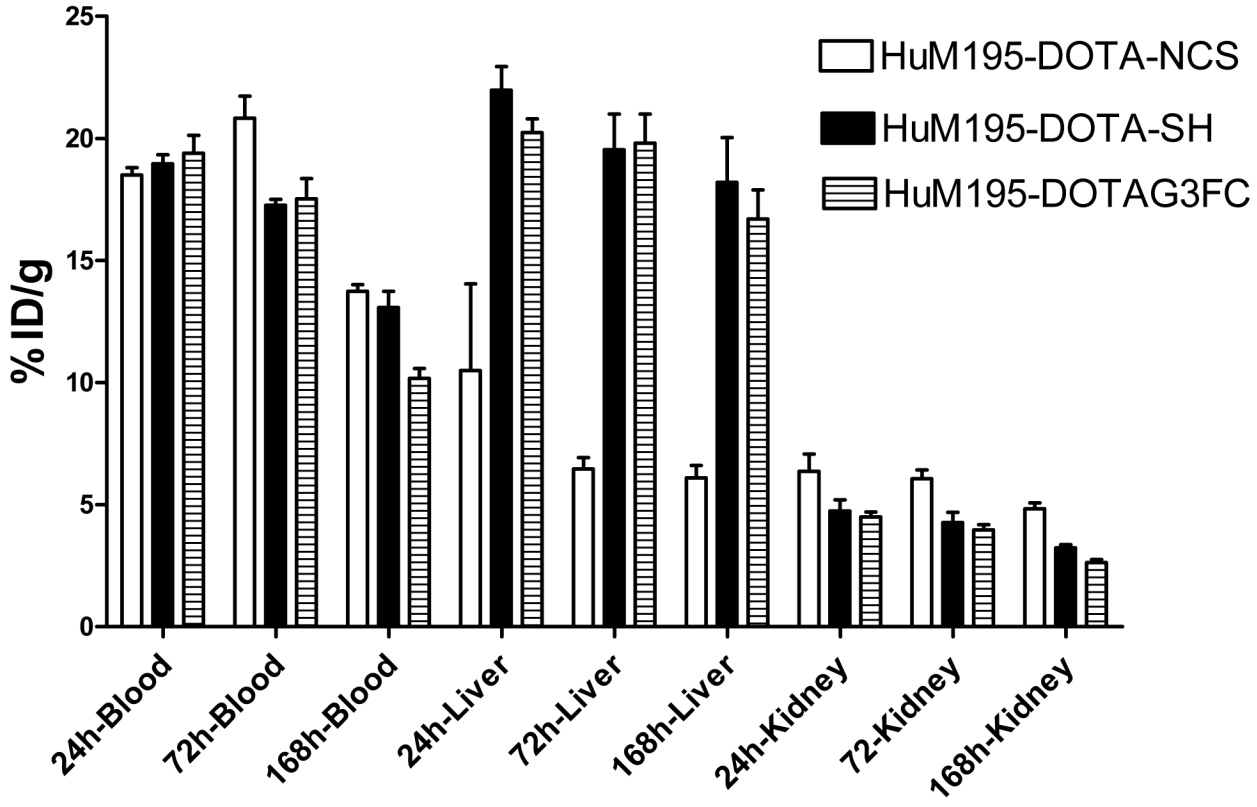

Figure 3.
Comparison of the biodistribution in mice of the RICs HuM195-DOTA-NCS **9**, HuM195-DOTA-SH **10**, and HuM195-DOTA-G3FC **11** labeled with ^{225}Ac.

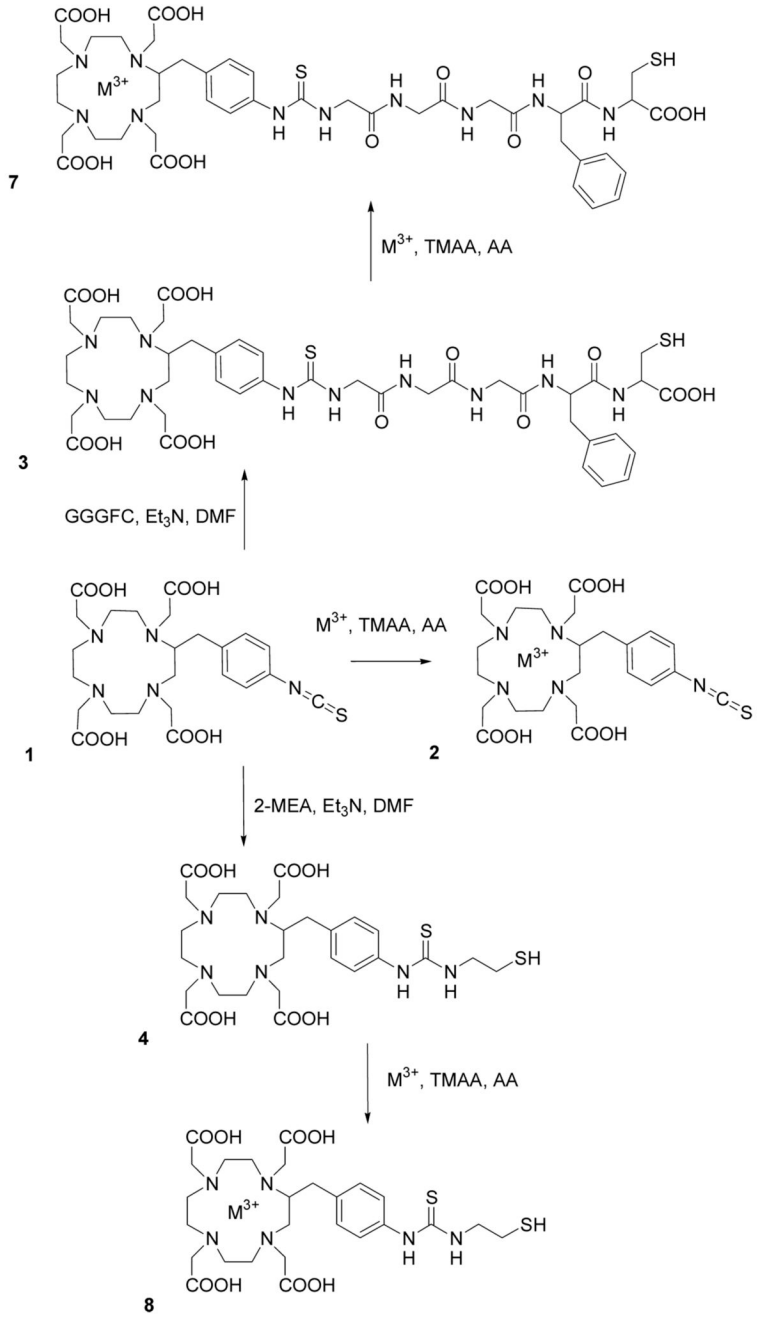

Scheme 1.
Bifunctional Chelating Agents.

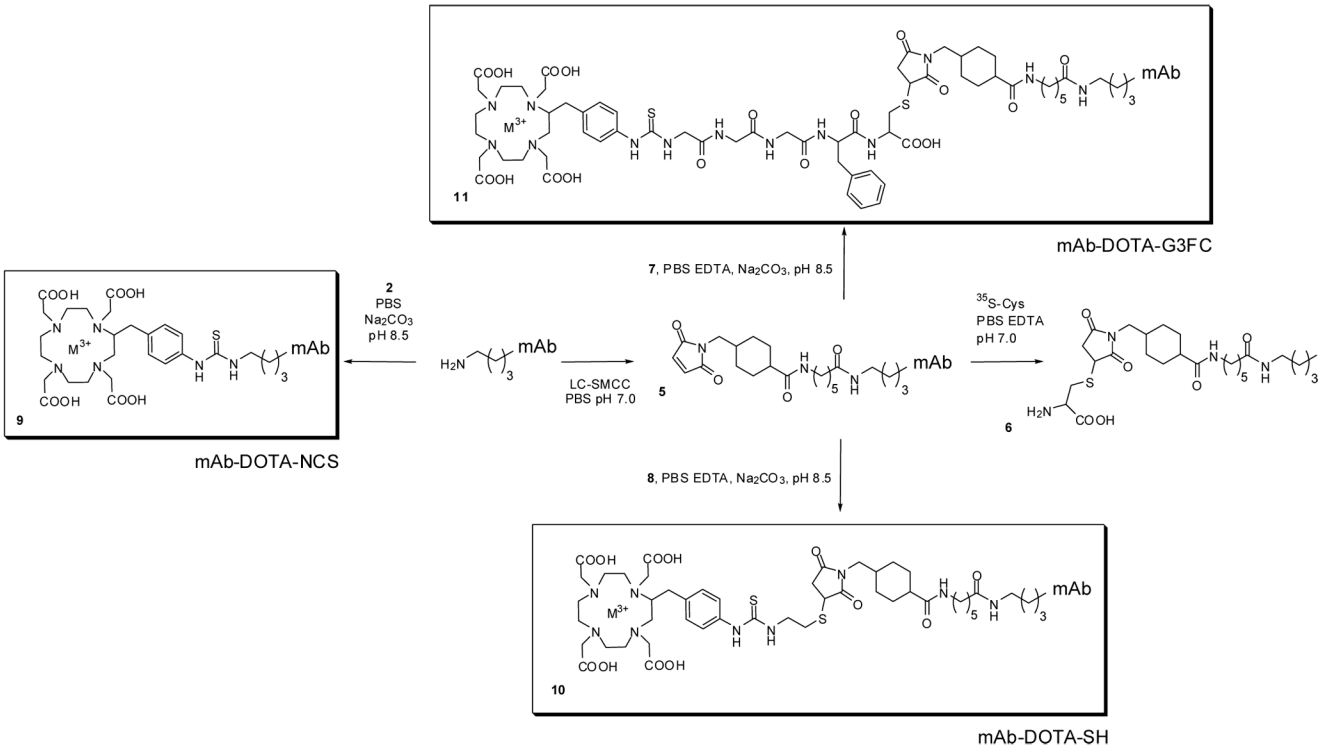

Scheme 2.
Radioimmunoconjugates.